

## Three-dimensional building response under seismic sequences

\*Jorge Ruiz-García<sup>1)</sup>

<sup>1)</sup> *Universidad Michoacana de San Nicolás de Hidalgo, Morelia, México*

<sup>1)</sup> [jruizgar@stanfordalumni.org](mailto:jruizgar@stanfordalumni.org)

### ABSTRACT

The objective of the ongoing research reported in this paper is to gain further understanding on the effect of seismic sequences on the three-dimensional (3D) building response. For this purpose, a 3D model of the three-story steel office building designed for the Los Angeles area as part of the SAC project (designated as the SAC LA 3-Story building) was subjected to different types of seismic sequences with different angles of orientation. It is first shown that a simplified two-dimensional model leads to different response than the 3D model. Furthermore, the amplitude of drift demands depended on the angle of orientation of the mainshock and the seismic sequence. Particularly, results obtained in this investigation indicate that far-field mainshock near-fault aftershocks trigger larger inelastic drift demands, which makes necessary to take into account this seismic scenario for structures located in seismic regions.

### 1. INTRODUCTION

There is a consensus among the earthquake engineering community that damage in structural elements, and some drift-sensitive nonstructural components, are primarily the result of lateral displacement demands induced by earthquake ground shaking in the structure. As a consequence, modern performance-based assessment methodologies for evaluation of existing structures (e.g. FEMA 356 2000) are based on the estimation of peak lateral displacement demands that man-made structures could suffer under seismic excitation. However, man-made structures located in seismic regions are not exposed to a single seismic event (i.e. mainshock), but also to a seismic sequence consisting on foreshocks, mainshock and aftershocks. For example, after the mainshock ( $M_w=8.8$ ) on February 27, 2010 that struck the central-southern region of Chile, 306 aftershocks having magnitudes greater than 5.0 were recorded between February 27 and April 26. Among them, 21 aftershocks had magnitude greater than 6.0. Thus, there is still a need of understanding the response of structures subjected to a seismic sequence of mainshock-aftershocks.

---

<sup>1)</sup> Professor of Civil Engineering

In the last 10 years, it has been an increasing interest at studying the effect of mainshock-aftershock seismic sequences on the response of civil engineering structures. Some studies have been focused on the nonlinear response of single-degree-of-freedom (SDOF) systems (e.g. Amadio 2003, Hatzigeorgiou 2009, Hatzigeorgiou 2010), while others in the response of multiple-degree-of-freedom (MDOF) systems (e.g. Fragiaco 2004, Lee 2004, Li 2007, Ruiz-Garcia 2008, Hatzigeorgiou 2010, Ruiz-García 2011, Faisal 2013). Most of the previous studies employed artificial seismic sequences instead of real (i.e. as-recorded) mainshock-aftershocks sequences to evaluate the seismic response. They employed artificial sequences using the mainshock acceleration time-history as a seed for simulating the following aftershocks using the following approaches: 1) back-to back, or repeated, approach (e.g. Amadio 2003, Fragiaco 2004, Hatzigeorgiou 2010, Faisal 2013); or 2) randomized approach (e.g. Luco 2004, Li 2007, Hatzigeorgiou 2010). The first approach consists on repeating the as-recorded mainshock as an artificial aftershock, which assumes that the ground motion features such as amplitude, frequency content, and strong motion duration of the mainshock and aftershock(s) are the same. The second approach consists on selecting a set of as-recorded mainshocks, and generating artificial sequences by selecting a mainshock and using the remaining mainshocks, once at a time, as an artificial aftershock.

It should be noted that although previous studies developed extensive analytical studies and provided information on the effect of seismic sequences on the response of structures, the use of artificial seismic sequences could lead to misunderstand the response of structures under real seismic sequences. Furthermore, with exception of the work done by Faisal (2013), all previous investigations on this subject have looked at the effect of seismic sequences on 2D analytical models, which means that the bi-directional effect of the sequences was neglected. It is worth noting that previous investigations on the three-dimensional (3D) building response have noted that the response of a 3D model is different to that of the corresponding simplified 2D model (e.g. MacRae 2000). These differences arise from the fact that the contribution of interior frames (e.g. gravity frames in the American practice), the contribution of orthogonal exterior moment resisting frames, among other factors, are not considered in a 2D analysis. However, MacRae (2000) highlighted that the 2D response not always lead to a larger response, as it might be expected, than the 3D response. Thus, there is still a need of investigating the response of 3D structures under real (i.e. as-recorded) mainshock-aftershock sequences.

The main purpose of this paper is to gain further understanding on the effects of real (i.e. as-recorded) mainshock-aftershock seismic sequences in the 3D response of buildings, which imply that the bi-directional attack of the sequences is taken into account in the analysis. First, four types of seismic sequences are identified from recorded events, highlighting that Far Field-Near Fault seismic sequences could have damaging effects on structures. After that, a well documented three-story steel office building designed for the Los Angeles area is analyzed under seismic sequences having different angles of orientation with respect to the X-direction of the building.

## 2. THREE-DIMENSIONAL STEEL FRAME CONSIDERED IN THIS STUDY

### 2.1 Building description

For the purpose of examining the influence of the angle of incidence of seismic sequences in the nonlinear response of buildings, selection of an adequate structure is highly important. Unlike other studies focused on the influence of the angle of incidence in simplified 3D models (i.e. one-story models, or one-bay multi-story models) this investigation chose a well-documented three-story multi-bay steel structure particularly designed for the SAC project to evaluate the performance of typical steel office buildings in Los Angeles area prior to the 1994 Northridge earthquake (Gupta 1999). The building was named the SAC LA 3-Story building, which has 6-by-4 bays with perimeter frames that include both steel moment resisting frames (SMRF) and gravity frames as shown in Fig. 1. Although the building is unsymmetrical, the lateral stiffness in each direction is similar, which lead to similar fundamental periods of vibration in both directions ( $T_X=0.99s$  and  $T_Y=0.94s$ , obtained from modal analyses). It should be noted that the frame in the X-direction of the building (N-S direction in the original design), shown in Fig. 2, has been extensively studied for several researchers. This exterior frame includes both SMRF's and gravity frame. Detailed information about the design process and member sizes can be found elsewhere (e.g. Gupta 1999).

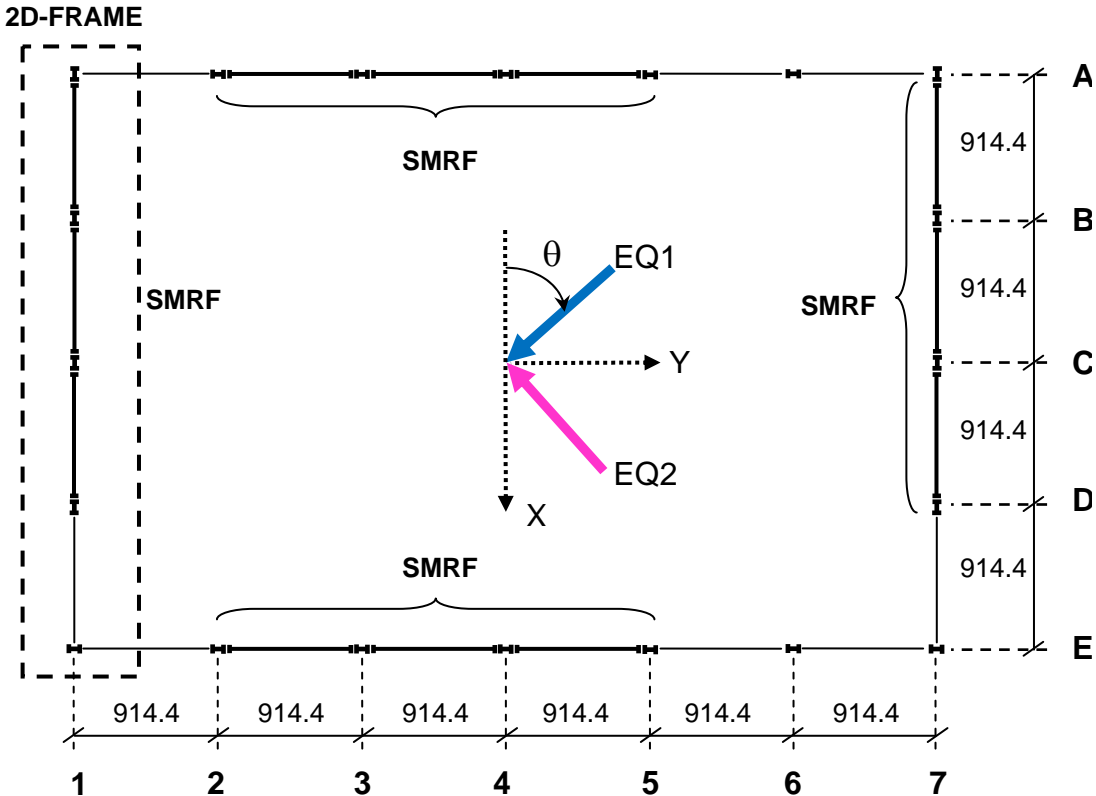


Fig. 1 Plan view of the SAC- LA 3-Story building considered in this study (units in cm)

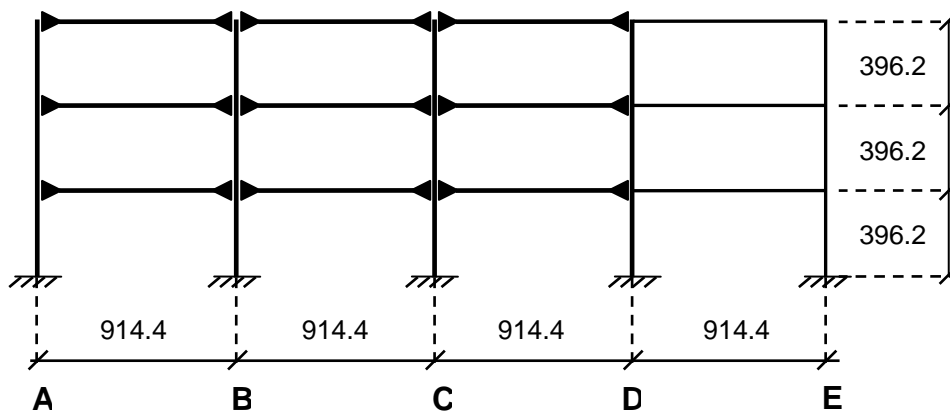


Fig. 2 Elevation (X-direction) of the 3-story perimeter SMRF (units in cm)

### 2.2 Modeling

In this investigation, a three-dimensional (3D) centerline model of the selected three-story structure was developed using the nonlinear dynamic analysis computer program RUAUMOKO3D (Carr 2009a). Only the perimeter frames were modeled as shown in Fig. 1, while the interior columns (i.e. gravity columns) and beams were omitted in the 3D model. Rigid diaphragm behavior was assumed at each floor. Additional interior fictitious columns (i.e. they do not provide additional lateral strength and stiffness to the 3D model) were included to carry vertical (gravity) loading of the building. Similarly, a two-dimensional (2D) centerline model of an exterior frame in the X-direction, as shown in Fig. 2, was developed with the computer program RUAUMOKO2D (Carr 2009b) for comparing its seismic response with the 3D model. The 2D model represents half of the building and it has an additional fictitious column. The fictitious column carries the vertical (gravity) loading from the rest of building (i.e. vertical loading carried by the interior gravity columns) and is attached to the exterior frame model through rigid frame elements to experience the same lateral deformation at each floor. However, the fictitious column does not provide the additional lateral stiffness from the interior gravity columns.

For the 2D and 3D models, beams (both in the SMRF and the gravity frames) and columns were modeled as frame elements which concentrate their inelastic response in plastic hinges located at their ends. A non-degrading bilinear moment-curvature relationship with strain-hardening ratio equal to 1% that considers axial load-flexural bending interaction was considered to model the hysteretic behavior of the steel columns. The beam behavior was modeled through a bilinear moment-curvature relationship with strain-hardening ratio equal to 1% that includes strength degradation due to fracture according to what has been discussed in Filiatrault (2001). Flexural moment capacity for beams and columns was determined using actual yield strength capacity of 337.8 MPa (49.2 ksi) and 399.9 MPa (57.6 ksi), respectively. However, additional strength and stiffness due to floor slab contribution in beams was neglected. The bending strength provided by the shear connections of the gravity beams (e.g.

beams between lines D and E in Fig. 2) was explicitly considered in both models. It was assumed that the shear connection provides 20% and 10% of the expected moment capacity in the positive and negative direction, respectively, as can be seen in Fig. 3.

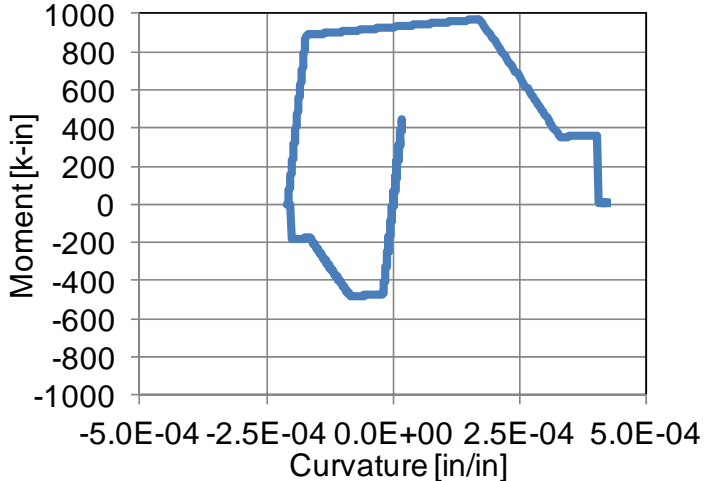


Fig. 3 Moment-curvature hysteretic behaviour assumed for shear (gravity) connections (beams between lines D and E in Fig. 2)

Before conducting dynamic analyses, nonlinear static (pushover) analyses were carried out to investigate the expected reserve of lateral strength in the 3D model with respect to the 2D model. Fig. 4 shows a comparison of the capacity curves obtained for both models in the X-direction. It can be seen that the models have similar lateral stiffness, but the 3D model has base shear capacity in excess of about 20% with respect to the 2D model, which is consistent with MacRae (2000).

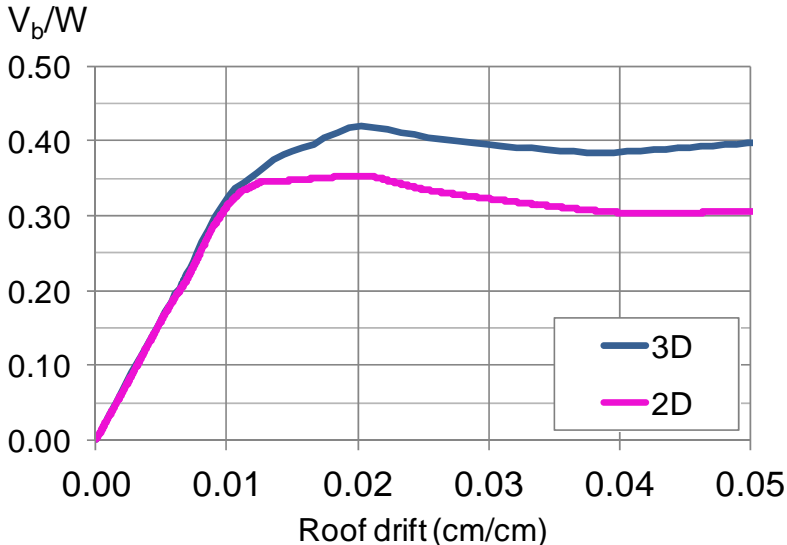


Fig. 4 Capacity curves for the 2D and 3D models corresponding to the X-direction

### 3. SEISMIC SEQUENCES CONSIDERED IN THIS STUDY

#### 3.1 Types of seismic sequences

Man-made structures located in earthquake-prone regions are not exposed to a single seismic event, but also to a *seismic sequence* consisting of foreshocks, the mainshock (i.e. the event with the largest earthquake magnitude) and aftershocks. It should be noted that the energy released after a mainshock event in a certain fault could trigger another mainshock in a nearby fault that could affect the same region. Therefore, for the purpose of analyzing the seismic response of structures, we could refer to a *seismic sequence* as the seismic event consisting of a mainshock earthquake ground motion and the subsequent (i.e. in time) largest aftershock earthquake ground motion, or a subsequent mainshock earthquake ground motion triggered in the site of interest. However, as it will be discussed later, assembling two mainshock earthquake ground motions from very different seismic events (i.e. active region, fault rupture mechanism, etc.) for the purpose of generating artificial seismic sequences is not an adequate approach.

Available strong motion databases, such as the Pacific Earthquake Engineering NGA Database (PEER 2013) and the Center for Engineering Strong Motion Data (CESMD 2013), among others, provide a good opportunity for identifying acceleration time-histories of recorded mainshocks and their corresponding largest aftershock. From a database of 218 seismic sequences, that includes sequences from the 1994 Northridge earthquakes and the 2010/2011 New Zealand earthquakes that struck the Canterbury region, the following observations are given: 1) Aftershocks recorded in the near fault region also exhibit pulse-like features in the velocity time-history similar to the mainshock such as in the 1994 Northridge earthquakes (Ruiz-Garcia 2011), 2) some aftershock acceleration time-histories have larger peak ground acceleration than the corresponding PGA in mainshock acceleration time-histories, in spite of having smaller earthquake magnitude. Examples of the latter seismic scenario observed during the 1994 Northridge earthquakes are shown in Fig. 5 (right plots). The former seismic sequence scenario was observed in some stations during the 1985 Michoacan earthquakes (Ruiz-Garcia 2012), and very recently in the 2010/2011 New Zealand earthquakes (i.e. following the September 3, 2010 Canterbury earthquake (Mw=7.0), a strong aftershock (Mw=6.1) was felt on February 21, 2011 that hit the city of Christchurch). Fig. 5 (left plots) shows two seismic sequences recorded in the city of Christchurch. This seismic scenario can be partially explained since the stations were located at a shorter epicentral distance from the aftershock epicenter than that from the mainshock epicenter. This could be a consequence of what seismologists call “aftershock migration”, which means that the rupture of asperities and barriers in a fault (i.e. according to Aki (1984), they are strong patches of the fault plane that are resistive to breaking, which explains the irregular slip motion over a heterogenous fault plane) triggers aftershocks. That is, an asperity/barrier release the stress concentration caused by the mainshock in the surrounding area and, as a consequence, it triggers the aftershock. In fact, larger asperity areas are related to large earthquakes (e.g. Ruff 1983).

Table 1. Earthquake ground motions recorded during the September 3, 2010 and the February 21, 2011 Canterbury earthquakes from the Center for Engineering Strong Motion Data (2012)

Station ID	Station name	Date (MODYYR)	Comp.	D [km]	PGA [cm/s <sup>2</sup> ]	Tm [s]
DFHS <sup>1</sup>	Darfield High School	030910	S17e	9.0	449.7	0.46
		022211	S17e	49.0	63.1	0.42
		030910	S73w	9.0	479.8	0.43
		022211	S73w	49.0	48.1	0.47
CACs <sup>2</sup>	Christchurch Canterbury Aero Club	030910	N40E	29.0	178.1	0.67
		022211	N40E	18.0	182.1	0.57
		030910	N50W	29.0	196.7	0.57
		022211	N50W	18.0	213.5	0.40
CMHS <sup>3</sup>	Christchurch Cashmere High School	030910	N10E	36.0	232.7	0.82
		022211	N10E	6.0	388.9	0.82
		030910	S80E	36.0	243.6	0.48
		022211	S80E	6.0	347.7	0.79
CHHC <sup>3</sup>	Christchurch Hospital	030910	N01W	36.0	194.1	1.78
		022211	N01W	8.0	329.2	0.94
		030910	S89W	36.0	149.8	0.94
		022211	S89W	8.0	353.9	1.14
CBGS <sup>3</sup>	Christchurch Botanic Gardens	030910	N89W	36.0	146.6	0.80
		022211	N89W	9.0	519.1	1.05
		030910	S01W	36.0	170.9	1.30
		022211	S01W	9.0	422.3	0.79
CCCC <sup>3</sup>	Christchurch Cathedral College	030910	N64E	38.0	224.5	0.98
		022211	N64E	6.0	473.9	1.18
		030910	N26W	38.0	198.3	1.38
		022211	N26W	6.0	359.7	1.16
SHLC <sup>3</sup>	Shirley Library	030910	S40W	39.0	171.5	0.76
		022211	S40W	9.0	306.2	0.95
		030910	S50E	39.0	175.9	1.06
		022211	S50E	9.0	335.2	1.03

<sup>1</sup> Near Fault-Far Field sequence

<sup>2</sup> Far Field-Far Field sequence

<sup>3</sup> Far Field- Near Fault sequence

D=epicentral distance, PGA=Peak ground acceleration, Tm=mean period.

Therefore, based on the epicentral distance of the mainshock and corresponding largest aftershock, four types of seismic sequences can be identified as follows: 1) Far field-Far field (FF-FF), 2) Near fault-Near fault (NF-NF), 3) Far field-Near fault (FF-NF), 4) Near fault-Far field (NF-FF). As discussed above, the FF-NF scenario would be the most critical, since earthquake-resistant structures should have enough residual capacity after an “ordinary”, or far-field, earthquake ground motion to sustain a most likely stronger aftershock.

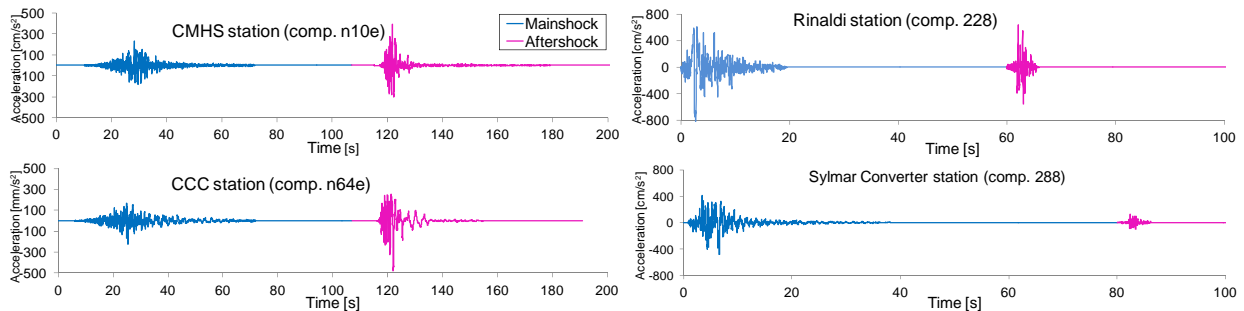


Fig 5. Examples of seismic sequences considered in this study from the 2010/2011 New Zealand earthquakes (left figures) and the 1994 Northridge earthquakes (right figures)

### 3.2 Seismic sequences selected in this study

In this investigation, five FF-NF seismic sequences were assembled from the September 3, 2010 Canterbury earthquake ( $M_w=7.0$ ) and the strong aftershock on February 21, 2011 ( $M_w=6.1$ ). Additionally one NF-FF and one FF-FF sequences were also included in the same set. Table 1 reports the list of seismic sequences and relevant ground motion features. The first component (reference component) listed in the table was varied an angle of incidence,  $\theta$ , while the second component was orthogonal. In addition, one NF-NF seismic sequence identified in the Rinaldi Receiving station during the 1994 Northridge earthquakes was considered as part of this investigation. In this sequence, the mainshock and aftershock records have peak ground acceleration equal to 809.2 and 639.0  $\text{cm/s}^2$ , respectively, while their mean periods are 0.76 and 0.35s, respectively. It should be noted that for performing dynamic analysis, there is a time-gap having zero acceleration ordinates between the as-recorded mainshock and the aftershock acceleration time-history to ensure that the systems reach its rest position.

## 4. RESPONSE UNDER SEISMIC SEQUENCES

### 4.1 Two-dimensional vs. three-dimensional response

In order to study the influence of mainshock-aftershock sequences in the response of existing steel frames, a series of nonlinear dynamic analyses were carried out for each frame model when subjected to the as-recorded seismic sequences. Dynamic time-history analyses were carried out using Newmark constant average acceleration

method with time step equal to 0.001s to enhance convergence. Rayleigh damping equal to 2% of critical was assigned to the first and second modes. During the analysis, local P-delta effects were included (i.e. large displacement analysis).

At a first stage, a comparison between the seismic response of the 3D building model in the X-direction analyzed with RUAUMOKO3D (Carr, 2009a) and a 2D frame (Fig.1) model analyzed with RUAUMOKO2D (Carr, 2009b) was conducted as part of this study. For this purpose, the sequences gathered in Rinaldi Receiving Station (RRS), comp. 228, and Christchurch Botanic Gardens Station (CBGS), comp. N89W, were employed for comparing the 2D and 3D response. Figs. 6a show a comparison between the height-wise distributions of peak inter-story drift, IDR, for the 3D and 2D models under the mainshock (M) and sequence (S) recorded at RRS. It should be noted that the mainshock earthquake ground motion triggered the peak inter-story drift demands, and, thus, only two lines are illustrated in Fig. 6a. This observation confirms previous findings that suggest that aftershocks recorded during the 1994 Northridge earthquake did not increase drift demands in this type of structures since their predominant period of the motion was significantly shorter than the fundamental period of vibration of the building (Ruiz-Garcia 2011). From the same figure, it can be observed that 3D model experienced significantly smaller IDR demands that those of the 2D model (i.e. the maximum inter-story drift at the bottom story in the 2D model is 3.3 times larger than that of the 3D model).

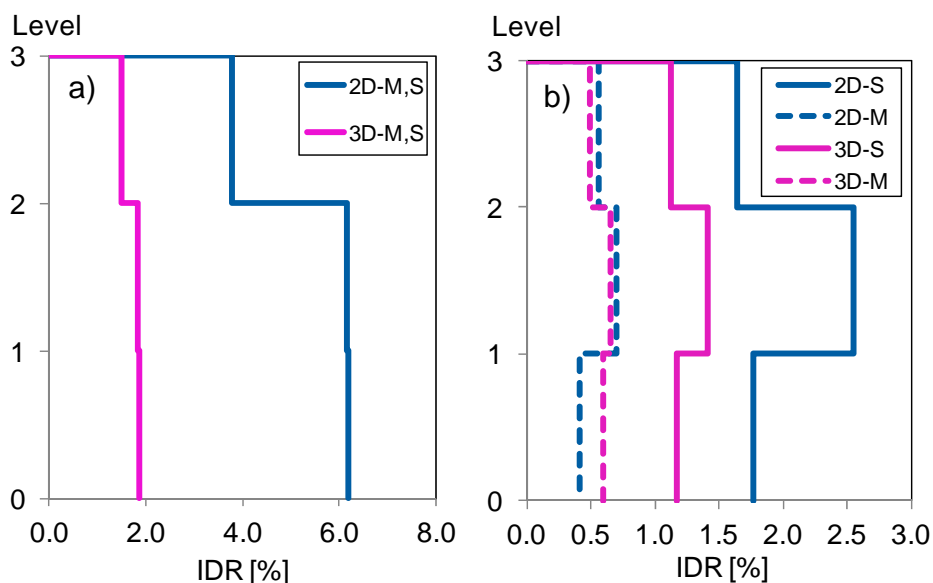


Fig. 6 Comparison of inter-story drift demand under mainshock (M) and sequence (S)) computed for the 2D and 3D frame models (X-direction): a) Rinaldi station (comp. 228), b) CBGS station (comp. N89W)

A similar comparison using the CBGS records is shown in Fig. 6b. It can be seen that both the peak IDR and their distribution along the height are very similar for both models under the mainshock, However, the response is significantly different under the sequence attack, with smaller peak inter-story drift demands induced in the 3D model

than those in the 2D model (e.g. maximum inter-story drift at all stories in the 3D models is 1.8 times larger than that of the 2D model). Therefore, these differences could be explained since the 3D has larger lateral strength capacity than that of the 2D model due to the contribution of the orthogonal moment resisting-frames, as illustrated in Fig. 1. Since the seismic performance of a structure to sustain an aftershock (or another seismic event) depends on its reserve capacity, neglecting the contribution of the orthogonal frames, and other three-dimensional effects, would overestimate the response under seismic sequences.

The influence of the frequency content of the aftershock (e.g. measured by the mean period of the ground motion,  $T_m$ ) can be inferred from comparing responses under both sequences. Note that IDR does not increase as a consequence of the aftershock in the RRS sequence unlike the increment under the CBGS sequence, although the peak ground acceleration of the aftershock recorded in the RRS station is greater than that recorded in the CBGS station about 23%. This could be explained since the aftershock in the RRS sequence has shorter  $T_m$  than that of the first-mode period of the building (“undamaged period”), but the  $T_m$  of the aftershock in the CBGS sequence is close to the first-mode period of the building. Furthermore, if the building experienced nonlinear behavior, its “damaged” period (i.e. period associated to loss of lateral stiffness) would be much larger than the  $T_m$  of the Rinaldi aftershock, and closer to the  $T_m$  of the CBGS aftershock. This important issue has been highlighted in Li (2007) and Ruiz-Garcia (2011, 2012).

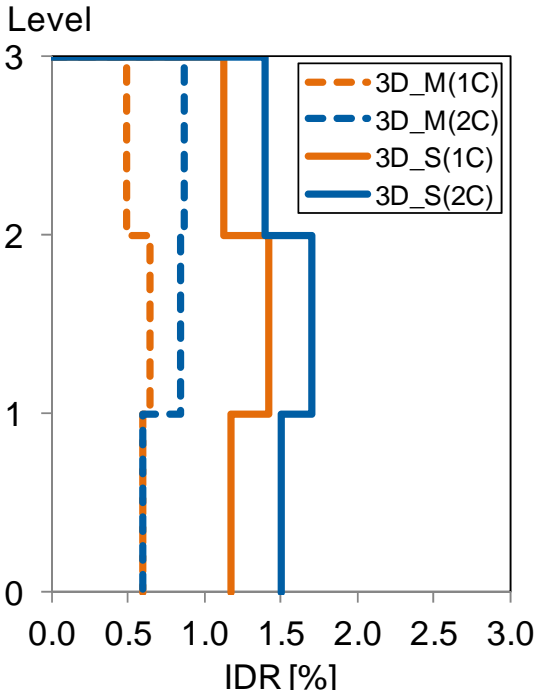


Fig. 7 Comparison of inter-story drift demand under mainshock (M) and sequence (S) for the 3D model (X-direction) taking into account one (1C) or two components (2C) of the earthquake ground motions recorded in the CBGS station

An interesting issue to examine in 3D response of the model is the amplitude and heightwise distribution of IDR under one- component or two-components (i.e. response under simultaneous action) of the earthquake ground motion excitation. Fig. 7 shows height-wise distribution of peak inter-story drift demand of the 3D model in the N-S direction under the mainshock and the sequence recorded in the CBGS station. For this case, it can be seen that IDR tends to be larger when both earthquake ground motion components take action simultaneously than when only one-component attack the 3D model. However, this difference is more notorious under the earthquake sequence.

#### *4.2 Influence of angle of incidence*

Fig. 8 illustrates the influence of the angle of incidence,  $\theta$ , in the peak inter-story drift demands of the 3D model under bi-directional seismic sequence excitation using both acceleration components recorded in the CBGS station. The response in the X- and Y-direction, as well as the total response using the square root of the sum of squares (SRSS) method, is plotted for five different angles of incidence. As can be expected, the response in each direction is different and the amplitude and difference depends on the angle of incidence. The largest total response is attained when  $\theta$  is equal to  $22.5^\circ$  while the shortest total response is reached when  $\theta$  is equal to  $67.5^\circ$ , having a difference of about 11%.

In addition, Fig. 9 shows a comparison of the variation of the total IDR triggered by the mainshock (M) and the sequence (S) for five different angles of incidence. It can be seen that the IDR due to the mainshock and aftershock, as well as its increment from the mainshock, depends on the angle of incidence. The largest increment in IDR occurred for an angle of  $90^\circ$  (however, this critical angle may change if the reference component is inverted, which was not examined in this study), followed by an angle of  $22.5^\circ$ .

The influence of the angle of incidence in the height-wise distribution of median peak inter-story drift demand of the 3D model when subjected to a set of 7 mainshock and sequence acceleration time histories is shown in Figs. 10, 11 and 12 for the X-direction, Y-direction and total response (SRSS), respectively. In general, it can be seen that the angle of incidence does not have a significant influence in the response under the mainshocks. However, it has more influence when the seismic sequence hit the 3D model, which is particularly true for the X-direction. For the X-direction and total response, the largest and shortest amplitude of median IDR is reached for angles of incidence of  $22.5^\circ$  and  $67.5^\circ$ , which corresponds to the second story. The increment is about 32% in the response in the X-direction, while it is about 14% for the total response. It is important to note that the sequence gathered in the DFHS station did not increase drift demands, and the increment is mostly attributed to the remaining sequences.

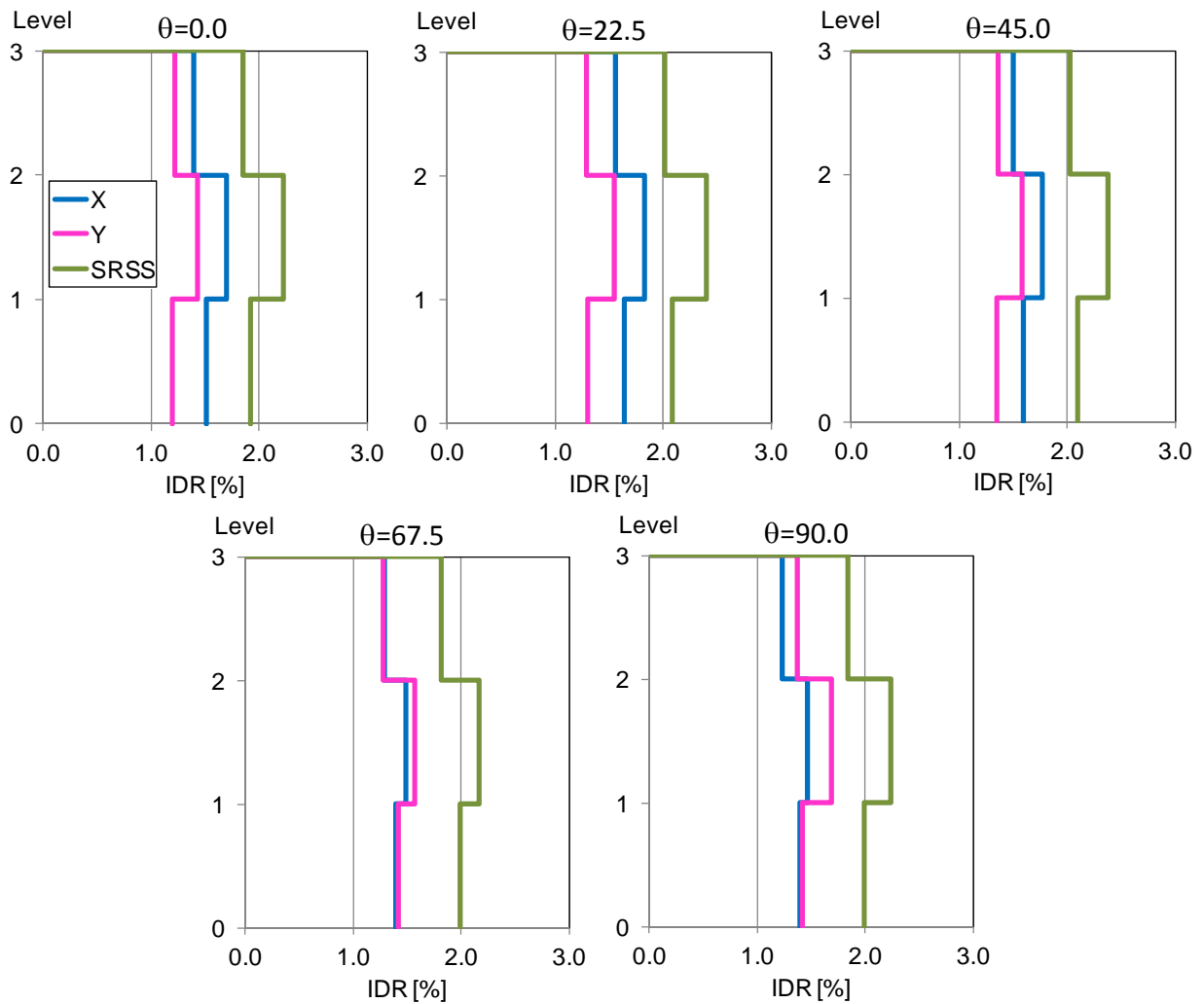


Fig. 8 Influence of angle of incidence in the inter-story drift demands (X-direction) of a 3D model under the bidirectional attack sequences recorded in the CBGS station

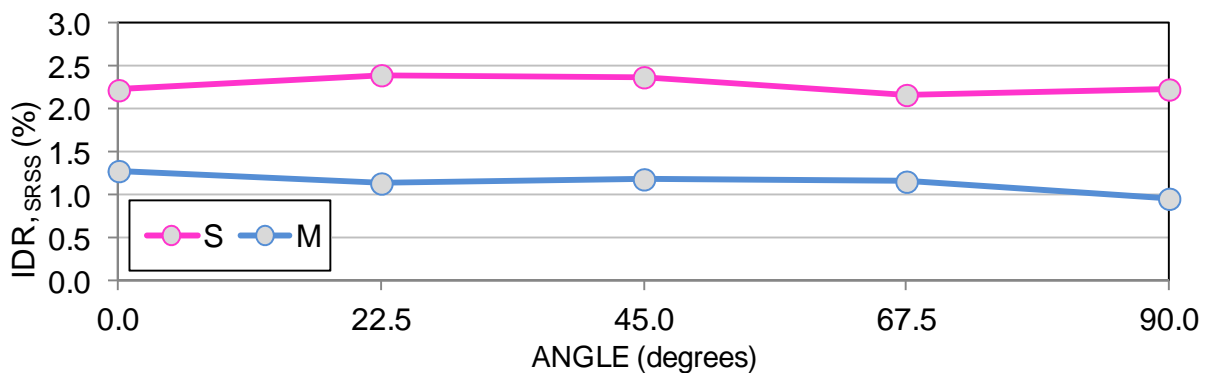


Fig. 9 Total IDR as a function of angle of incidence

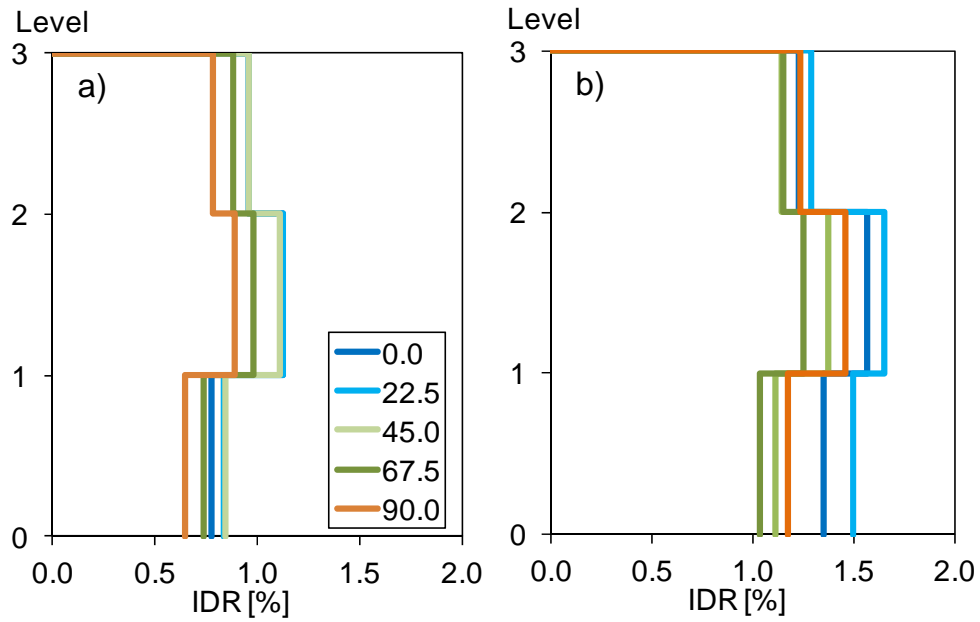


Fig. 10 Influence of angle of incidence in IDR (X-direction) of a 3D model under the bidirectional attack of a set of records gathered during the NZ earthquakes:  
a) mainshock, b) sequence

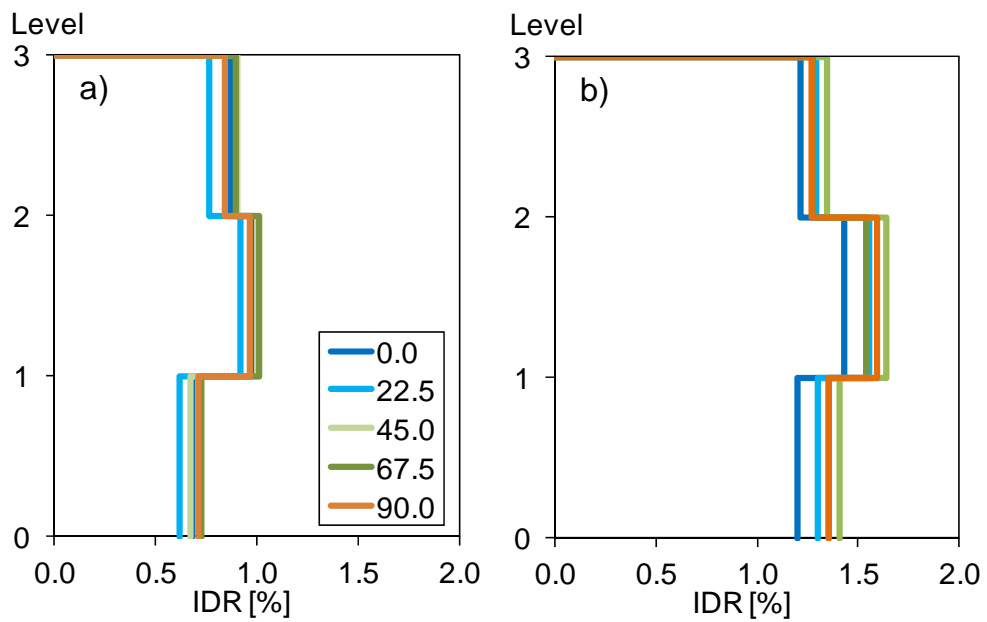


Fig. 11 Influence of angle of incidence in IDR (Y-direction) of a 3D model under the bidirectional attack of a set of records gathered during the NZ earthquakes:  
a) mainshock, b) sequence

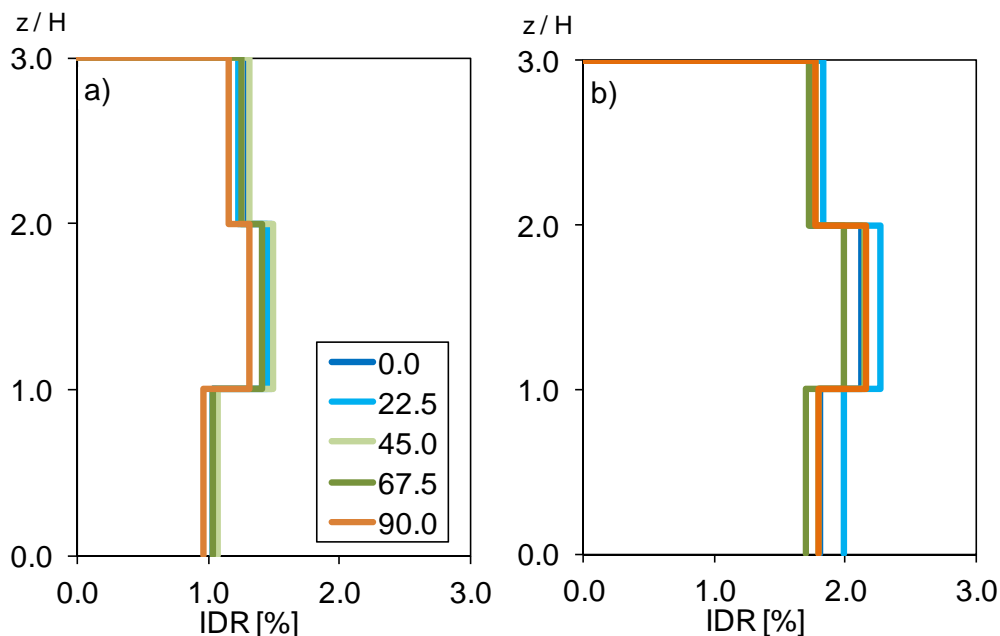


Fig. 12 Influence of angle of incidence in IDR (total response) of a 3D model under the bidirectional attack of a set of records gathered during the NZ earthquakes:  
a) mainshock, b) sequence

## 5. CONCLUSIONS

The influence of the angle of incidence in the peak drift response of a 3-story three-dimensional (3D) model subjected to real seismic sequences was discussed in this paper. Particularly, the 3D building response under Far Field-Near Fault sequences identified from the 2010/2011 New Zealand earthquakes was examined in this study. The following conclusions are drawn from this ongoing investigation:

As noted in previous studies, the two-dimensional (2D) and three-dimensional (3D) seismic response under earthquake excitation is different. Furthermore, if the building model experienced nonlinear behavior after the mainshock, the results obtained in this investigation suggest that the 3D seismic response under the following aftershock is very different with respect to the 2D response.

When subjected to orthogonal seismic sequences recorded during the 2010/2011 New Zealand earthquakes applied to different angles of incidence, it was shown that the angle of incidence has an effect on the largest interstory drift demands, particularly under the aftershock attack. The largest response was found at an angle of 22.5° with respect to the X-direction of the model. Therefore, this investigation highlights that a better understanding about the effect of seismic sequences should be envisioned looking at the three-dimensional response of buildings. Particularly, Far Field-Near Fault sequences lead to larger drift demands than those computed from the mainshock.

## ACKNOWLEDGEMENTS

The author would like to express his gratitude to the *National Council for Science and Technology* (CONACYT) in México for the financial support provided to develop the research reported in this paper through the project CB-2008-102721. Special thanks are given to the *Universidad Michoacana de San Nicolás de Hidalgo*.

## REFERENCES

- Aki, K. (1984), "Asperities, barriers, characteristic earthquakes and strong motion prediction", *J. of Geophysical Research*, **89**(B7): 5867-5872.
- Amadio, C., Fragiaco, M. and Rajgelj, S. (2003), "The Effects of repeated earthquake ground motions on the non-linear response of SDOF systems", *Earthq. Eng. Struct. Dyn.*, **32**, 291-308.
- CESMD (2012), Center for Engineering Strong Motion Data. <http://www.strongmotioncenter.org/>. Last access: 03/21/12
- Carr, A J. (2009a), RUAUMOKO3D. Volume 3: User manual for the 3-Dimensional version, Dept. of Civil Engineering, University of Canterbury, Christchurch, New Zealand.
- Carr, A J. (2009b), RUAUMOKO2D. Volume 2: User manual for the 2-Dimensional version, Dept. of Civil Engineering, University of Canterbury, Christchurch, New Zealand.
- Faisal, A., Majid, T.A. and Hatzigeorgiou, G. (2013), "Investigation of story ductility demands of inelastic concrete frames subjected to repeated earthquakes", *Soil Dyn. Earthq. Eng.*, **44**, 42-53.
- Federal Emergency Management Agency (2000). Prestandard and Commentary for the Seismic Rehabilitation of Buildings. Report FEMA 356, Washington, D.C.
- Filiatrault, A., Tremblay, R. and Wanitkorkul, A. (2001), "Performance evaluation of passive damping systems for the seismic retrofit of steel moment-resisting frames subjected to near-field ground motions", *Earthq. Spectra*, **17**(3), 427-456.
- Frangiaco, M., Amadio, C. and Macorini, L. (2004), "Seismic response of steel frames under repeated earthquake ground motions", *Eng. Struct.*, **26**, 2021-2035.
- Gupta, A. and Krawinkler, H. (1999), "Seismic demands for performance evaluation of steel moment resisting frame structures", Report TR-132, John A. Blume Earth. Eng. Ctr., Stanford University.
- Hatzigeorgiou, G. and Beskos, D.E. (2009), "Inelastic displacement ratios for SDOF structures subjected to repeated earthquakes", *Eng. Struct.*, **31**, 2744-2755.
- Hatzigeorgiou, G. (2010), "Ductility demand spectra for multiple near- and far-fault earthquakes", *Soil Dyn. Earthq. Eng.*, **30**, 170-183.
- Hatzigeorgiou, G.D. and Liolios, A.A. (2010), "Nonlinear behaviour of RC frames under repeated strong ground motions", *Soil Dyn. Earthq. Eng.*, **30**, 1010-1025.
- Lee, K. and Foutch, D.A. (2004), "Performance evaluation of damaged steel frame buildings subjected to seismic loads", *J. of Struct. Engrg.*, **130**(4), 588-599.
- Li, Q. and Ellingwood, B.R. (2007), "Performance evaluation and damage assessment of steel frame buildings under main shock-aftershock sequences", *Earthq. Eng. Struct. Dyn.*, **36**, 405-427.

- Luco, N., Bazzurro, P. and Cornell, C.A. (2004), "Dynamic versus static computation of the residual capacity of mainshock-damaged building to withstand an aftershock", *Proceedings 13th. World Conference on Earthquake Engineering*, Paper No. 2405, Vancouver .
- MacRae, G., and Mattheis, J. (2000), "Three-dimensional steel building response to near-fault ground motions", *J. Struct. Engrg.*, **126** (1), 117-126.
- Pacific Earthquake Engineering Research Center PEER Strong Motion Database. [www/http://peer.berkeley.edu/nga/](http://peer.berkeley.edu/nga/). Last access: 07/20/2010.
- Ruff, F. and Kanamori, H. (2003), "The rupture process and asperity distribution of three great earthquakes from long-period diffracted P-waves," *Physics of the Earth and Planetary Interiors*, **31**, 202–230.
- Ruiz-García, J., Moreno, J.Y. and Maldonado, I.A. (2008), "Evaluation of existing Mexican highway bridges under mainshock-aftershock seismic sequences", *Proceedings of the 14th. World Conference on Earthquake Engineering*, Beijing, China, Paper 05-02-0090.
- Ruiz-García, J. and Negrete-Manriquez, Juan. C. (2011), "Evaluation of drift demands in existing steel frames under as-recorded far-field and near-fault mainshock-aftershock seismic sequences", *Eng. Struct.*, **33**, 621-634.
- Ruiz-García, J. (2012), "Mainshock-aftershock ground motion features and their influence in building's seismic response", *J. Earth. Eng.*, **33**, 621-634.